

Full Length Research Paper

Crystal size effect on the photoluminescence of calcium aluminate doped Mn^{2+} nanocrystals

Jubu P. Rex^{1*}, Abutu A. Nathan¹ and Mbah Vitalis²

¹Department of Physics, University of Agriculture, Makurdi, Benue State, Nigeria.

²Department of Science Laboratory Technology, Federal Polytechnic, Nasarawa, Nasarawa State, Nigeria.

Received 15 August, 2015; Accepted 2 October, 2015

Research into finding environmentally friendly, efficient and economic viable nanophosphors is still ongoing as the incorporation of radioactive substances into phosphors to improve their short time luminescence poses serious environmental concern. The present paper investigates the effect of particle size on the, morphology and photoluminescence of environmentally friendly $CaAl_2O_4: Mn^{2+}$ nanocrystals. The phosphor was prepared by the high temperature reaction technique. X-ray diffraction analysis revealed monoclinic structure. Average crystal size of the unpassivated nanomaterial (CAU) was found to be higher (41.49 nm) than that of the passivated (CAP) one (34.81 nm). Photoluminescence investigation at 345 nm excitation showed emission wavelengths that match Mn^{2+} emission. Both the emission color and intensity of the nanocrystals were observed to be crystal-size dependent with high luminescence intensity and deep blue emission peaks coming from CAP; while low luminescence intensity, prominent violet peaks and a weak blue emission peak were registered on CAU. Investigation of the samples responds to different excitation wavelengths revealed that both materials received corresponding colour emission and maximum intensity at 465 nm excitation.

Key words: Photoluminescence, morphology, passivation, fluorescence phosphor.

INTRODUCTION

Last two decades have witnessed a rapid advancement in various techniques for the fabrication of nanoparticles (Senapati et al., 2013). The interest in semiconductor nanoparticles is justified by the fact that their fundamental physical and chemical properties can be very different from those of bulk materials. The advantages of nanoparticles over their bulk counterparts include small particle size with large surface area, improved optical, electrical and mechanical properties. According to Kelvil (2013), nanoparticles have the advantage over bulk

materials due to their surface plasmon response, enhanced Rayleigh scattering and surface enhanced Raman scattering in metal nanoparticle and their quantum size effect in semiconductors and supermagnetism in magnetic materials. The II-VI nanostructures with their distinct optical and electrical properties due to their two-dimensional confinement and anisotropic shape have become potential candidates for application in electronics, optoelectronics, lasers and environmental control (Sugaderan, 2013; Kenanakis et al., 2007; Mou et

*Corresponding author. E-mail: jubu_raphael@yahoo.com

Author(s) agree that this article remain permanently open access under the terms of the [Creative Commons Attribution License 4.0 International License](https://creativecommons.org/licenses/by/4.0/)

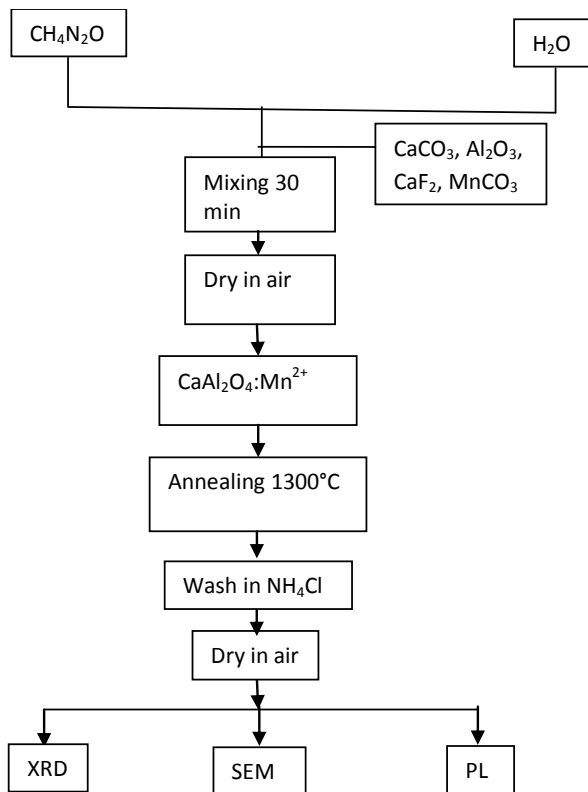


Figure 1. Summary of synthesis and characterization of nanoparticles.

al., 2012).

Nanostructures have been successfully synthesized by various methods like chemical or physical vapour deposition, thermal evaporation, magnetron sputtering, laser ablation, hydrothermal method, spray pyrolysis, catalyst-mediated organization, electrodeposition, homogeneous precipitation, solvothermal synthesis, sonochemical process and sol-gel process (Amita and Srivastava, 2011). Amongst these methods, monocalcium aluminate (CaAl_2O_4) have been successfully prepared by solution combustion method (Vijay et al., 2007; Nguyen et al., 2004; Ali, 2011; Dejene et al., 2010), hydrazine assisted self-combustion (Satapathy and Mishra, 2014), sol-gel and solid state method (Toumas et al., 2012; Jagjeet et al., 2002; Madhukumar et al., 2006; Bo et al., 2005; Rivas et al., 2004). But the use of urea in solid state synthesis has been negligible.

The role of urea ($\text{CH}_4\text{N}_2\text{O}$) in the development of blue-emitting monocalcium aluminate nanoparticles was to tailor the structural, morphological and luminescence properties of the nanomaterial. Urea finds several roles in the preparation of nanomaterials. For example, urea is used as a flux by many researchers to promote the formation of a good crystalline phase system (Haranath et al., 2010). Urea is used as a popular fuel for producing highly uniform, complex oxide ceramic powders with

precisely controlled stoichiometry (Christine et al., 2010). Exothermic redox reaction occurs between fuel and oxidizers (nitrates) (Toniolo et al., 2005) which generate high temperature in the reaction.

In the present paper, we investigated the morphology, crystal structure and size, and photoluminescence emission behavior of $\text{CaAl}_2\text{O}_4:\text{Mn}^{2+}$ nanocrystals prepared by slurry. Solid state diffusion is the most popular method for the preparation of nanophosphors even at commercial scale (Kartik et al., 2012). The monocalcium aluminate was doped to introduce new properties by changing the mass transport properties (Saeid et al., 2012). Fluorescence phosphors like CaAl_2O_4 , $\text{BaMgAl}_{12}\text{O}_{19}$, $\text{SrAl}_2\text{B}_2\text{O}_7$ finds application in light emitting devices, plasma display panels, medical lamps and fluorescent lamps (Haranath et al., 2010). Our success in this research is anchored on the reduction of crystallite size of the nanoparticles synthesized by the high temperature reaction using urea as passivating agent; knowing that reduced particle size and hence large surface area, enhances photoluminescence mechanism by providing reinforcement and catalytic effect. (Ali, 2011) asserts that when the diameter of a particle is reduced the band gap is blue-shifted due to the effect of quantum confinement.

MATERIALS AND METHODS

The requisite materials used for the successful execution of the research include the following. Calcium carbonate (CaCO_3), aluminum oxide (Al_2O_3), manganese carbonate (MnCO_3), calcium fluoride (CaF_2), ammonium chloride (NH_4Cl), pure urea ($\text{CH}_4\text{N}_2\text{O}$), distilled water and muffle furnace. All chemicals are of analytical grade and were used without further purification. Chemicals were purchased from Suzhou Yacoo Chemical Reagent Co. Ltd, China.

In this present study, the nanomaterial was prepared according to the chemical formula $\text{Ca}_{0.2}\text{Al}_2\text{O}_4:\text{Mn}_{0.004}$. All the precursors were of analytical grade and were used without further purification. In order to study the effect of urea on the nanoparticles, two samples were prepared. Sample CAU was prepared by slurring CaCO_3 , Al_2O_3 , CaF_2 , and MnCO_3 in distilled water for 20 min and left to dry in air. The resulting powder was grounded into fine particles using pestle and mortar. Muffle furnace was used to maintain the crucibles containing the samples at 1300°C for 1 h in order to cause changes in the physical and chemical constitution of the nanomaterials and also to drive off carbon dioxide. Sample CAP was synthesized in a similar way though by slurring the precursors in a solution of 2.0g urea in order to reduce the crystal size of the nanomaterial. Both samples, CAU and CAP were washed in 0.25l of water using 4.0g ammonium chloride to extract the impurities and left to dry in air.

Characterization of the nanocrystals was carried out using X-ray diffractometer PW3050/60 at the Sheda of Science and Technology Abuja, Nigeria. The nature and form of the material was studied using scanning electron microscope an oxford instrument at the Amadu Bello University Zaria, Nigeria. The photoluminescence property was examined using photoluminescence spectrometer model Perkin-Elmer LS-55 domiciled at National Centre for Nanostructured Materials (CSIR), Pretoria, South Africa.

The chemical reactions leading to the synthesis process are as presented in equations 1 to 3 while the flowchart showing summary of the synthesis is presented in Figure 1.

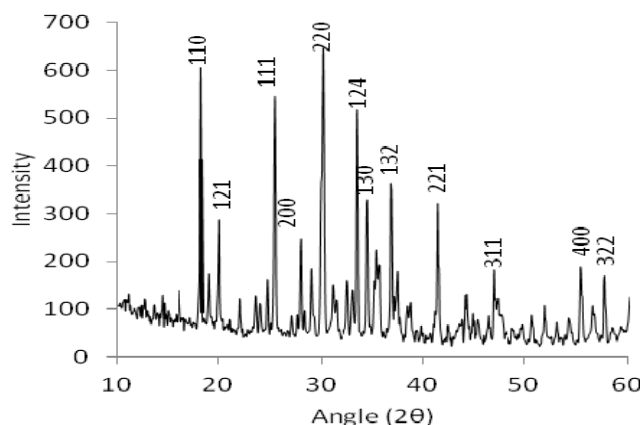


Figure 2a. XRD pattern of CAP

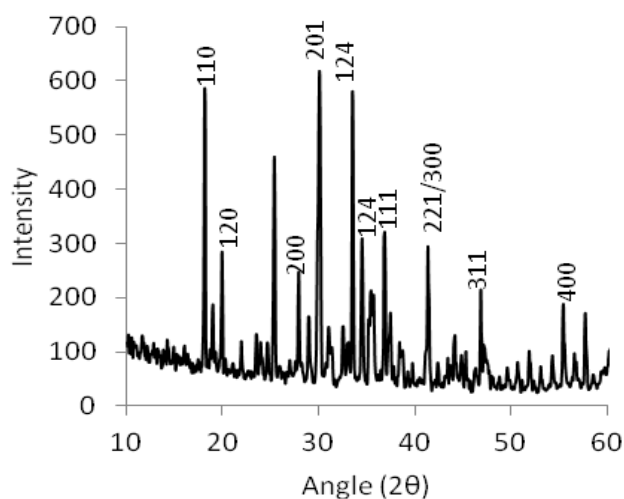
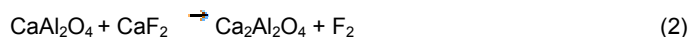
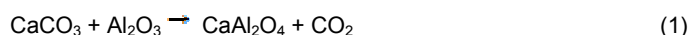


Figure 2b. XRD pattern of CAU.



Crystal size of the nanoparticles was calculated using Debye Scherrer formula which states that

$$D = \frac{0.9\lambda}{\beta \cos\theta} \quad (4)$$

where D is the crystallite size, λ is wavelength of the X-ray source in nm, β is the full width at half maximum (FWHM) in radians, and θ is the angle of diffraction in radians.

The strain of the nanoparticles was calculated from Stokes-Wilson equation:

$$\epsilon_{str} = \frac{\beta \sin\theta}{4} \quad (5)$$

where β is FWHM (in radian) and θ is diffraction angle (in radians).

The amount of defect in the sample can be estimated from:

$$\delta = \frac{1}{2D} \quad (6)$$

where D is average particle size and δ is dislocation density.

RESULTS AND DISCUSSION

Crystal structure and size determination

The X-ray diffraction patterns of the synthesized $\text{CaAl}_2\text{O}_4 \cdot \text{Mn}^{2+}$ nanocrystals is shown in Figures 2a and b. Six prominent peaks were observed in the diffractograms around 2θ values of 33.63, 30.08, and 18.22° corresponding to (124), (201), (110) for CAU and 30.15, 25.53 and 18.29° corresponding to (220), (111), (110) for CAP (Table 1). All the planes can be indexed to CaAl_2O_4 . Structural identification of the nanomaterials from the XRD revealed monoclinic structure of the Mn^{2+} doped calcium aluminate nanophosphor. The high intensity of the peaks reveals the high crystallinity of the synthesized nanomaterials (Arunachalam, 2012). Average crystal size calculated from three prominent peaks show that the unpassivated sample, CAU, has the largest crystal size of 41.49 nm as a result of low strain and dislocation in the crystals; while the passivated sample, CAP, has 34.81 nm due to high dislocation and strain in the crystals. This is an indication that the presence of urea assists in the dissolution and combustion of the particles leading to increased crystal defect and strain. Urea has been applied in the preparation of nanomaterials using solution combustion synthesis (Qui et al., 2007; Krsmenovic et al., 2007). All these led to a homogeneous system with blended morphology and enhanced luminescence with reduced particle size. This of course is evident in the present paper.

Surface morphology study

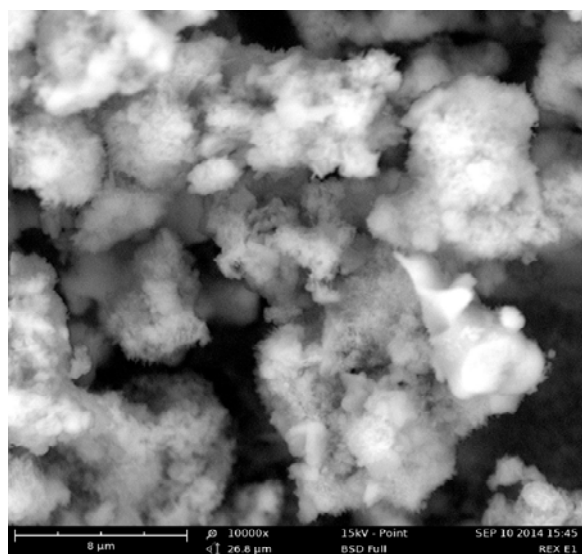
The SEM micrograph unveils the foamy nature of the passivized CAP with wide particle distributions. The unpassivized CAU reveals the cluster spherical nature of the crystals interconnected by nanorods which could be due to poor dissolution of the particles (Figure 3a and b).

Photoluminescence studies

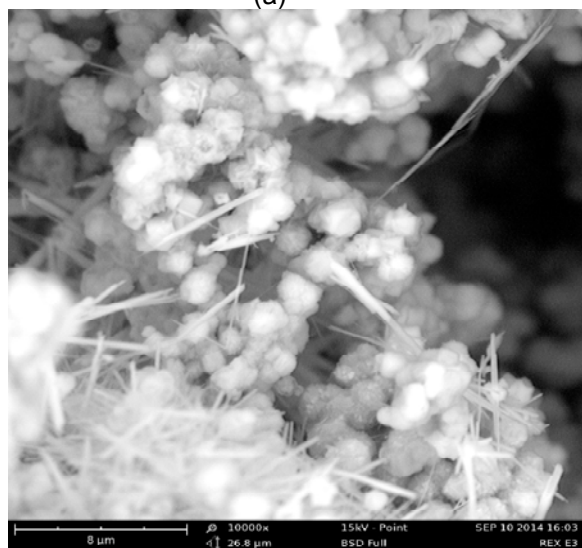
The ability of the nanoparticles to absorb incident energy and convert it into visible radiation was confirmed by PL investigation. Photoluminescence emission spectrum at 345 nm excitation shows three distinct peaks centered at 406, 454 and 493 nm for CAP with the maximum intensity obtained at 454 nm (Figure 4). Four distinct peaks were

Table 1. The structural data of sample CAP and CAU.

Sample ID	2 θ (°)	FWHM (°)	Interplanar Spacing 'd' (Å)	Plane (hkl)	Intensity	Average crystal size (nm)	Average dislocation density (lines/m)	Average crystal strain
CAP	30.15	0.3296	2.964	220	644.0	34.81	9.87×10^{-4}	2.82×10^{-1}
	25.53	0.1978	3.500	111	542.2			
	18.29	0.1978	4.869	110	604.6			
CAU	33.57	0.1978	2.673	124	574.5	41.49	8.73×10^{-4}	2.3×10^{-1}
	30.08	0.3296	2.969	201	617.1			
	18.22	0.1319	4.884	110	583.7			



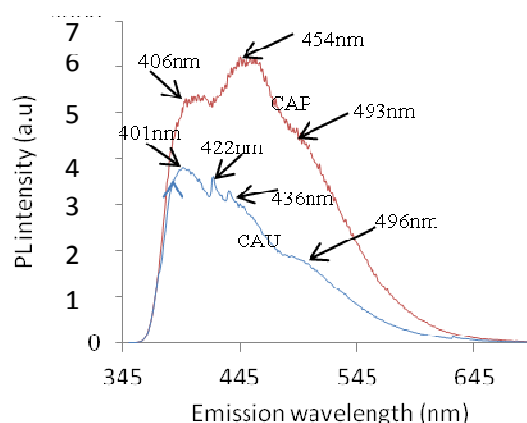
(a)



(b)

Figure 3. The SEM micrograph analysis of sample (a) CAP (b) CAU nanocrystals.

obtained at 401, 422, 436 and 496nm respectively for CAU with the maximum intensity coming from 401 nm. All

**Figure 4.** Photoluminescence emission spectra of the samples at 345 nm excitation.

the peaks are in good agreement with the well-known Mn^{2+} emission transitions (Jubu et al., 2015). The emission wavelengths indicate characteristic blue emission which is typical of Mn^{2+} . Similar blue emission wavelengths were also obtained by Lin et al. (2008). The luminescent intensity of the thermal treated products varied appreciably with the presence of urea as CAP has the highest luminescence intensity. The emission intensity of the nanomaterials vary with crystal size such that CAU with high crystal size has a low emission intensity. According to (Dhlamini, 2008) the emission colors of phosphors vary with crystallite size. This is evident on CAU with dominant violet (380–450) nm emission peaks, and a low blue (450–495) nm emission peak due to high particle size of 41.49 nm; and CAP with deep blue emission peaks as a result of reduced particle size of 34.81 nm (Jagjeet et al., 2002) obtained blue-green emission on the phosphor at 254 nm UV excitation. The blue emission originates from the electron-hole recombination of self-trapped exciton (Yit-Tsong, 2002). As can be seen on Figure 5, the samples showed unique responds to different excitation wavelengths. The CAP sample has low responses at 320 and 395 nm. The presence of urea seemingly enhanced the sensitizers of the CAP sample giving them better responses to a wide range of excitation wavelengths as a result of reduced

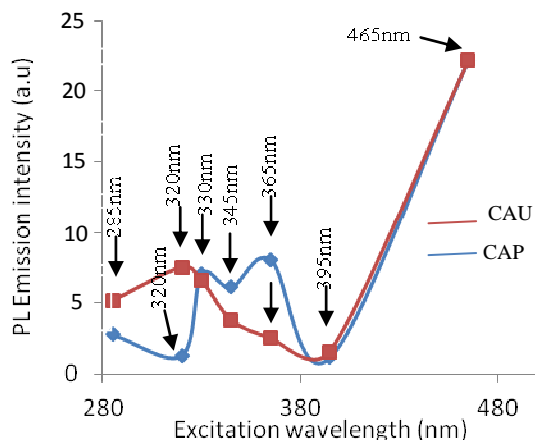


Figure 5. Plot of excitation wavelengths against highest emission intensities.

particle size. The emission intensities of CAP fluctuates between 285 and 395 nm UV excitation doses but increased sharply at 465 nm excitation giving rise to the highest emission intensity.

The CAU sample, without urea, and with high crystal size responded poorly between 330 and 395 nm excitation. This is probably due to the high crystallite size and hence increased band gap leading to decrease photoluminescence intensity as a result of separation of exciton wave functions with the activator (Diane, 2002). The hindered overlap reduces the energy transfer rate from the exciton to the impurities and as a result the non-radiative decay rate is increased and therefore the photoluminescence efficiency is decreased. A sharp responds by sensitizers is also recorded at 465 nm excitation on CAU. The samples respond differently to different excitation wavelengths as a result of variation in their particle sizes. Equivalent responses are recorded at 330, 395 and 465 nm respectively. The significant effect of particle size on photoluminescence emission intensity of the samples is quenched at the highest excitation wavelength, 465 nm, which gave the sensitizers of both samples a similar highest responds.

Conclusion

The manipulation of morphology and particle size by urea, and the effect of crystal size on the photoluminescence of manganese doped calcium aluminate nanocrystalline material was successfully carried out. Study revealed that the presence of urea reduced the average crystallite size of CAU from 41.49 to 34.81 nm for CAP, with the prepared $\text{CaAl}_2\text{O}_4:\text{Mn}^{2+}$ samples being monoclinic in structure. The SEM micrograph of CAU revealed spherical particles connected by nanorods, while the SEM image of CAP unveiled the foamy nature of the nanocrystals. The emission color and

intensity of the nanocrystals were observed to be crystal-size dependent with high luminescence intensity and deep blue emission peaks recorded on CAP; while low luminescence intensity, prominent violet peaks and a weak blue emission peak were registered on CAU. Particle size was observed to have no effect on photoluminescence emission intensity at 465 nm excitation wavelength.

Conflict of Interest

The authors have not declared any conflict of interest.

REFERENCES

- Ali HW (2011). Preparation and Properties of Long Afterglow CaAl_2O_4 Phosphors Activated by Rare Earth Metal Ions. M.Sc Thesis, University of the Free State, Republic of South Africa, pp. 10–121.
- Amita V, Srivastava AK (2011). Sol-gel Derived Nanostructural Zinc Oxide for Bright Luminescence in Ultraviolet and Visible Spectral Region. *Indian J. Chem.* 50:1697–1702.
- Arunachalam L (2012). The Role of Sintering in the Synthesis of Luminescence Phosphor. Sintering of Ceramics, In Tech Publishers, Thandulam, Chennai, India, pp. 321-337.
- Bo L, Chaoshu S, Zeming Q (2005). Potential White-Light Long-Lasting Phosphors: Dy^{3+} -Doped Aluminate. *Appl. Phys. Lett.* 86:191111-191113.
- Christine KS, Samson AN (2010). Effect of Fuels on the Combustion Synthesis of NiAl_2O_4 Spinel Particles. *Iranian J. Mater. Sci. Eng.* 7(2):36-38.
- Dejene FB, Bem DB, Swart HC (2010). Synthesis and Characterization of $\text{CaAl}_2\text{O}_4:\text{Eu}^{2+}$ Phosphor Prepared Using Solution-Combustion Meth. *J. Rare Earth* 28:272-276.
- Dharamini MS (2008). Luminescence Properties of Synthesized PbS Nanoparticles. PhD Thesis, University of the Free State, South Africa.
- Diane KW (2002). Particle Size Dependence on the Luminescence Spectra of $\text{Eu}^{3+}:\text{Y}_2\text{O}_3$ and $\text{Eu}^{3+}:\text{CaO}$. PhD Dissertation, Virginia Polytechnic Institute and State University, Blacksburg, Virginia, pp. 1-154.
- Haranath D, Pooja S, Harish C, Anwar A, Nitesh B, Halder SK (2010). Role of Boric Acide in Synthesis and Tailoring the Properties of Calcium Aluminate Phosphors. *Mater. Chem. Phys.* 101:163-164.
- Jagjeet k, Nemana S, Beena J, Vikas D, Ravi S, Huma NB (2002). TL Glow Curve Study, Kinetics, PL and XRD Analysis of Mn^{2+} Doped CaAl_2O_4 Phosphors. *J. of Min. and Mat. Character Engin.* 11:1081-1084.
- Jubu PR, Onoja AD, Echi IM (2015). Doping Concentration Dependence of the Luminescence of Mn^{2+} Activated Calcium Aluminate Nanoparticles. *Res. J. Phys. Sci.* 3(3):1-4.
- Kartik NS, Dhoble SJ, Swart HC, Kyeongsoon P (2012). Phosphate Phosphors for Solid-State Lighting. Springer Verlag Berlin Heidelberg, pp. 1-75
- Kelvil WG (2013). Green Technology for Nanoparticles in Biomedical Applications. CAB International, 1-108
- Kenanakis G, Androulidaki KE, Savvakis C, Katsarakis N (2007). Photoluminescence of ZnO Nanostructures Grown by Aqueous Chemical Growth Technique. *Superl. Microst.* 42:473–478.
- Krsmenovic R, Morozov V, Lebedev O, Polizzi S, Speghini A, Bettinelli M (2007). Structural and Luminescence Investigation on Gadolinium Gallium Garret Nanocrystalline Powders Prepared by Solution Combustion Synthesis. *Nanotechnology* 18:325604-325613.
- Lin L, Min Y, Chao SS, Weiping Z (2008). Luminescence properties of a new red long-lasting phosphor: $\text{MgSiO}_4:\text{Dy}^{3+}, \text{Mn}^{2+}$. *J. Alloys Comp.* 455:327-330.
- Madhukumar K, Rajendra KB, Ajith PKC, James J, Elias TS,

- Padmanabhan V, Nair CMK (2006). Thermoluminescence Dosimetry of Rare Earth Doped Calcium Aluminate Phosphors. *Bull. Mat. Sci.* 29(2):119 -122.
- Mou P, Umapada P, Justo MG, Jimenez Y, Felipe PR (2012). Effects of Crystallization and Dopant Concentration on the Emission Behavior of $\text{TiO}_2\text{:Eu}$ Nanophosphors. *Nanosc. Res. Let.* 7(1):1-12.
- Nguyen NT, Nguyen MS, Phun TD (2004). Photoluminescence Characteristics of the $\text{CaAl}_2\text{O}_4\text{:Eu}^{2+}$ Co-doped with Dy^{3+} Synthesized by Combustion Method." *Int. J. Chem. Mat. Res.* 2(8):7575–80.
- Qui Z, Zhou Y, Lu M, Zhang A, Ma Q (2007). Combustion Synthesis of Long-Persistent Luminescent $\text{MAl}_2\text{O}_4\text{:Eu}^{2+}, \text{R}^{3+}$ (M = Sr, Ba, Ca, R = Dy, Nd and La). *Nanop. Lumines. Mech. Res.* 55:2620-2626.
- Rivas JM, De'Aza AH, Pena P (2004). Synthesis of CaAl_2O_4 from Powders –Particle Size Effect." *J. Eur. Cera. Soc.* 25:3269-3279.
- Saeid K, Jalal R, Ehsan M, Mahmoud A, Arash D (2012). Synthesis and Characterization of Cr-Doped Al_2O_3 Nanoparticles Prepared Via Aqueous Combustion Method. *Casp. J. Appl. Sci. Res.* 1(13):16-22.
- Satapathy kk, Mishra GC (2014). Hydrazine Assisted Self-combustion Synthesis of $\text{CaAl}_2\text{O}_4\text{:Eu}^{2+}$ Phosphor and its Mechanoluminescence Characterization." *Int. J. Sci, Basic Appl. Res.* 16:188-196.
- Senapati US, Jha DK, Sarkar D (2013). Green Synthesis and Characterization of ZnS Nanoparticles. *Res. J. Phys. Sci.* 1(7):1-6.
- Sugaderan S (2013). Synthesis, Structural, and Dielectric Properties of Zinc Sulfide Nanoparticles. *Int. J. Phys. Sci.* 8(21):11-21.
- Toniolo J, Lima M, Takimi A, Bergmann C (2005). Synthesis of Alumina Powders by the Glycine-Nitrate Combustion Process. *Mater. Res. Bull.* 40(3):561-569.
- Toumas A, Jorma, Hogne, Mika L, Janne N (2012). Comparison of Sol-Gel and Solid State Prepared Eu^{2+} Doped Calcium Aluminates." *Mat. Sci.* 20(1):16-19.
- Vijay S, Natarajan V, Jun-Jie Z (2007). Luminescence and EPR Investigations of Mn Activated Calcium Aluminate Prepared via Combustion Method. *Sci. Direct Opt. Mat.* 30:468 -472.
- Yit-Tsong C (2002). Size Effect on the Photoluminescence Shift in Wide Band-Gap Materials: A Case Study of SiO_2 -Nanoparticles. *Tamkang J. Sci Eng.* 5(2):99 -106.